

On the Bilayer Coupling in the Yttrium-Barium Family of High Temperature Superconductors

A. J. Millis* ^a and H. Monien ^b

^a *Bell Laboratories*

Lucent Technologies

700 Mountain Avenue

Murray Hill, NJ 07974

^b *Physikalisches Institut*

Universität Bonn

Nußallee 12

D-53115 Bonn

Germany

Abstract

We derive the expressions needed to interpret experiments relating to interplane magnetic coupling in $\text{YBa}_2\text{Cu}_3\text{O}_{6+x}$ and related materials, and use the results to interpret measurements of the optical magnon energy in $\text{YBa}_2\text{Cu}_3\text{O}_{6.2}$ and of the NMR “cross-relaxation” rate in $\text{Y}_2\text{Ba}_4\text{Cu}_7\text{O}_{15}$. We estimate $J_{\perp} \sim 14$ meV in both materials, and $\chi_{\text{max}}/\mu_B^2 \sim 100$ states/eV-Cu in $\text{Y}_2\text{Ba}_4\text{Cu}_7\text{O}_{15}$ at $T = 100\text{K}$. We show that there is at present no obvious contradiction between the results of a widely-used analysis of NMR experiments and the results of neutron scattering experiments in the Y-Ba system.

We argue that the 41 meV excitation observed in superconducting $\text{YBa}_2\text{Cu}_3\text{O}_7$ is a collective mode pulled down below the superconducting gap by interactions, and that the observed antisymmetry under interchange of planes follows from the non-negligible value of J_{\perp} .

I. INTRODUCTION

In the yttrium-barium (Y-Ba) family of high temperature superconductors the basic structural unit is a “bilayer” consisting of two CuO_2 planes; the bilayers are separated by CuO chains and the coupling between bilayers is very weak. Neutron scattering¹ and more recently NMR experiments² have shown that the Cu spins on adjacent planes in a bilayer are coupled. Intra-bilayer coupling has been shown theoretically to lead to a “spin gap”^{3–7} similar to that observed⁸ in NMR experiments on underdoped members of the Y-Ba family. In view of the great importance of the spin gap phenomenon, a quantitative analysis of the spin dynamics of a bilayer is desirable. In this communication we provide this analysis and use it to interpret NMR and neutron scattering experiments. Our new results include (a) a calculation of the quantum renormalization of the optic spin-wave gap in the $S = \frac{1}{2}$ Heisenberg bilayer, (b) the proper analysis of the NMR “cross-relaxation” experiment², (c) refined estimates of the inter-bilayer coupling and in-plane antiferromagnetic susceptibility, (d) a demonstration that there is no obvious contradiction between the results obtained from an analysis of the NMR data in terms of the “MMP” model^{9,10} and the results obtained from neutron scattering¹¹ and (e) an improved understanding of a theory for the 41 meV peak observed¹² in neutron scattering experiments on superconducting $\text{YBa}_2\text{Cu}_3\text{O}_7$. A brief account of this work has been presented elsewhere¹³

Focus on the two planes of a bilayer, and neglect coupling to other bilayers. Label the spin degrees of freedom by an index $a = 1, 2$ distinguishing planes, and a site index i . Consider the susceptibility

$$\chi^{ab}(q, \omega) = \int_0^\infty dt e^{i(\omega t + \vec{q} \cdot (\vec{R}_i - \vec{R}_j))} \langle [\vec{S}_i^a(t), \vec{S}_j^b(0)] \rangle. \quad (1)$$

Here \vec{S} is the usual spin $\frac{1}{2}$ operator. Because of the symmetry under exchange of planes, χ^{ab} has only two independent components, $\chi^{11}(q, \omega) = \chi^{22}(q, \omega)$ and $\chi^{12}(q, \omega) = \chi^{21}(q, \omega)$. The two independent components of χ may be taken to be the even and odd (under the interchange of planes) components $\chi_{\text{even,odd}} = \chi_{11} \pm \chi_{12}$. The main goals of this paper are to relate experimental observations to χ^{11} and χ^{12} and these to Hamiltonian parameters.

The rest of this paper is organized as follows. In section II we derive an expression for the optic spin wave gap for the bilayer Heisenberg model and use the result to obtain from data^{14,15} an expression for the bilayer coupling J_{\perp} in $\text{YBa}_2\text{Cu}_3\text{O}_{6.2}$. In section III we formulate, solve and apply to data a model for the spin dynamics of a metallic (but non-superconducting) bilayer, obtaining estimates for J_{\perp} , the antiferromagnetic susceptibility, and the temperature dependence of the correlation length. In section IV we extend the model to the superconducting state and show that it accounts naturally for the observation of the superconducting state 41 meV peak observed in $\text{YBa}_2\text{Cu}_3\text{O}_7$ ¹² and the lack of measurable signal in the normal state. Our results provide a new interpretation of a previously published numerical calculation¹⁶, explain why the effect was not seen in another calculation¹⁷ and show that an objection raised by other workers¹⁸ is not valid. Section V is a conclusion.

II. BILAYER HEISENBERG MODEL

In this section we estimate the optic magnon energy of the bilayer Heisenberg model defined by the Hamiltonian

$$H = \frac{1}{2}J \sum_{i\delta} \vec{S}_i^{(a)} \cdot \vec{S}_{i+\delta}^{(a)} + J_{\perp} \sum_i \vec{S}_i^1 \vec{S}_i^2 \quad (2)$$

Here $a = 1, 2$ labels planes, i labels sites of a two dimensional square lattice, δ labels the four in-plane nearest neighbors of a site, and the \vec{S}_i are the usual $S = \frac{1}{2}$ spin operators.

We solve Eq. 2 via the Schwinger boson method¹⁹, which has been shown²⁰ to give very accurate estimates for the quantum renormalization of the single-plane $S = \frac{1}{2}$ Heisenberg model. We previously used the Schwinger boson method to analyze the quantum disordered phases of Eq. 2²¹. The analysis presented here amounts to an extension of that work to the ordered phase; we therefore omit all details of the derivation of the equations, and mention only necessary notation and new features.

In brief, to use the Schwinger boson method one introduces Bose fields $b_{i\alpha}^{+(a)}$ so that $S_{i\alpha}^{(a)} = b_{i\alpha}^{\dagger(a)} \vec{\sigma}_{\alpha\beta} b_{i\beta}^{(a)}$. The fields are subject to the constraint $(2S + 1) = \sum_{\alpha} b_{i\alpha}^{\dagger(a)} b_{i\alpha}^a$. The

$\vec{S} \cdot \vec{S}$ interactions become four-boson interactions, which one decouples with Hubbard-Stratonovich fields Q (for the in-plane interaction J) and Δ (for the between planes interaction J_\perp). One must also introduce a Lagrange multiplier μ to enforce the constraint. The mean field equations are given in Eqs. 2.9 of Ref.²¹ and are rewritten here for convenience:

$$\begin{aligned} \int \frac{d^2k}{(2\pi)^2} \frac{\mu}{\omega_k} \left[1 + 2b\left(\frac{\omega_k}{T}\right) \right] &= 1 + 2S \\ \int \frac{d^2k}{(2\pi)^2} \frac{(Q\gamma_k + \Delta)\gamma_k}{\omega_k} \left[1 + 2b\left(\frac{\omega_k}{T}\right) \right] &= Q/2J \\ \int \frac{d^2k}{(2\pi)^2} \frac{(Q\gamma_k + \Delta)\gamma_k}{\omega_k} \left[1 + 2b\left(\frac{\omega_k}{T}\right) \right] &= 2\Delta/J_\perp \end{aligned} \quad (3)$$

Here $\gamma_k = -\frac{1}{2}(\cos k_x + \cos k_y)$, $\omega_k = \sqrt{\mu^2 - (Q\gamma_k + \Delta)^2}$ and $b(x) = (e^x - 1)^{-1}$. In the limit $J_\perp \rightarrow 0$ these equations reduce those studied by Arovas and Auerbach¹⁹, except that in our conventions Q is four times larger than in theirs. At low T for parameters such that the ground state is ordered at $T = 0$ one has

$$\mu^2 = (Q + \Delta)^2 + (\kappa/2)^2 \quad (4)$$

with inverse correlation length κ given by

$$\kappa = \kappa_0 \exp(-2\pi\rho_s/T). \quad (5)$$

Equation 5 defines the spin stiffness ρ_s .

In the $T \rightarrow 0$ limit the integrals in Eqs. 3 may be evaluated up to corrections of order T by noting that the terms proportional to $b(\omega_k/T)$ are dominated by the divergence as $\omega_k \rightarrow 0$ while in the terms proportional to 1 one may set $\kappa = 0$. If T is less than the optic mode gap one finds

$$\begin{aligned} Q &= 2J[2S + 1 - I_{oa} + I_{ob}] \\ \Delta &= \frac{1}{2}J_\perp[2S + 1 - I_{oa} + I_{oc}] \\ \rho_s &= \frac{1}{4}Q[2S + 1 - I_{oa}] \end{aligned} \quad (6)$$

Here $I_{oa,b,c}$ are respectively the $T = 0$ values of the first, second and third integrals on the left hand sides of Eqs. 3. They depend upon the ratio Δ/Q and in the limit $\Delta \ll Q$ are

$$\begin{aligned} I_{oa} &= 1.39 - \frac{2}{\pi} \sqrt{\frac{\Delta}{Q}} + O\left(\frac{\Delta}{Q}\right) \\ I_{ob} &= 0.55 - \frac{2}{\pi} \sqrt{\frac{\Delta}{Q}} + O\left(\frac{\Delta}{Q}\right) \\ I_{oc} &= \frac{2}{\pi} \sqrt{\frac{\Delta}{Q}} + O\left(\frac{\Delta}{Q}\right) \end{aligned} \quad (7)$$

Expressions for dynamic susceptibilities are given in Appendix C of Ref.²¹. In the limit of interest here the absorptive parts are dominated by poles representing undamped spin waves. In the acoustic sector the dispersion is given by $\omega = \omega_k$ with k near $Q = (\pi, \pi)$. In the optic sector the dispersion for wavevectors near Q is given by $\omega = \omega_{k+Q}$. In particular the acoustic spin wave velocity is $c^2 = \frac{1}{2}Q(Q + \Delta)$ and the optic-mode gap $\omega_{opt} = 2\sqrt{\Delta Q}$. Neglecting terms of relative order Δ/Q we find $c = 2\sqrt{2}Z_c(S)JS$ and $\rho_s = 2Z_{\rho_s}(S)JS^2$ with $Z_c(\frac{1}{2}) = 1.16$ and $Z_{\rho_s}(\frac{1}{2}) = 0.71$, in agreement with previous work^{19,20}. [The factor of two in ρ_s occurs because each unit cell contains two *Cu* ions, one in each plane; for $T \ll \omega_{opt}$ the two planes move together].

The equation for Δ may be rearranged to read

$$J_{\perp} = \frac{\omega_{opt}^2}{8\rho_s + \frac{2}{\pi}\omega_{opt}} \quad (8)$$

If one takes the limit $J_{\perp}/\rho_s \rightarrow 0$ and sets $Z_{\rho_s} = 1$, this reduces to the usual $\omega_{opt} = 4\sqrt{JJ_{\perp}}S$.

Recent neutron scattering measurements^{14,15} have reported $\omega_{opt} \cong 70$ meV for $\text{YBa}_2\text{Cu}_3\text{O}_{6.2}$. Use of the canonical values $J = 100$ meV and $Z_{\rho_s} = 0.7$ implies $J_{\perp} \cong 14$ meV. Our value for J_{\perp} differs from that quoted in the experimental papers because those works assumed $Z_{\rho_s} = 1$ and neglected the second term in the denominator of Eq. 8. Some caution is necessary in using this value because the measurements were made on samples of nominal composition $\text{YBa}_2\text{Cu}_3\text{O}_{6.2}$. The effects of the extra 0.2 of oxygen might lead to substantial changes of Z_{ρ_s} from the ideal-system $Z_{\rho_s} \approx 0.7$ value.

We can also obtain from the formalism an expression for the strength of the spin-wave poles. In the regime of interest the momentum integrals are dominated by the infrared divergence at $\omega_k \ll T$; we find, for the susceptibility per plane,

$$\chi''(q, \omega) = \frac{16\pi\rho_s}{\omega_q} [\delta(\omega - \omega_q) - \delta(\omega + \omega_q)] \quad (9)$$

For the acoustic branch, $\omega_q = cq$; for the optic branch, $\omega_q = \omega_{opt}$. The prefactor may be written as $4\pi S\sqrt{2}Z_{\rho_s}/Z_c(qa)$ or (using $c^2 = \rho_s/\chi_{\perp}$) $4\pi S\sqrt{2}Z_{\chi}Z_c/(qa)$, where a is the lattice constant. This susceptibility is, up to an apparently omitted factor of Z_c , consistent with that given in Eq. 8 of¹¹. Those authors define χ as $\frac{1}{2\pi}\langle S^-S^+ \rangle$ and measure it per bilayer. The factor of two from S^-S^+ versus S^zS^z and the factor of two from bilayers leads to a difference of $\pi/2$ in our conventions.

III. METALLIC BILAYER

This situation is more complicated and less well defined than the insulating antiferromagnetic case because there is neither a generally accepted theory of the magnetic dynamics of a single layer nor a generally accepted theory of the interlayer coupling. One must therefore proceed phenomenologically. Despite the obvious limitations, we believe that this is worth doing because the spin dynamics of metallic cuprates are a subject of continuing interest and, as we shall show, recent measurements of interplane effects yield information about both the between-planes coupling and the in-plane spin dynamics.

Further analysis requires a model. We shall assume that the magnetic dynamics of a single plane may be described by a susceptibility $\chi_0(q, \omega)$ whose form we discuss further below. We also assume that the only interplane coupling is the magnetic one, $J_{\perp} \sum_i \vec{S}_i^{(1)} \cdot \vec{S}_i^{(2)}$. This is not an important restriction. Retaining the off-diagonal term χ_0^{12} in our formalism leads only to a modest renormalization of J_{\perp} , as shown also in¹⁶. Finally, we assume that the effects of J_{\perp} may be modeled via the RPA. Thus we write

$$\chi^{-1} = \begin{bmatrix} \chi_0^{-1}(q, \omega) & -J_{\perp} \\ -J_{\perp} & \chi_0^{-1}(q, \omega) \end{bmatrix}. \quad (10)$$

We further assume (as has been done in previous analyses of NMR in high T_c materials⁹) that $\chi_0(q, \omega)$ has the scaling form $\chi_0(q, \omega) = \chi_0 \xi^2 f(q\xi, \omega/\xi^z)$, where f is a scaling function normalized so that $f(0, 0) = 1$, z is the dynamical exponent, ξ is a correlation length measured in units of the lattice constant and \vec{q} is measured from an ordering wavevector \vec{Q} which for the present discussion is arbitrary. \vec{Q} is believed to be of the order of (π, π) in high T_c materials. From Eq. 10 we see that $\chi^{11}(q, \omega) = \chi_0(q, \omega)/(1 - (J_{\perp}\chi_0(q, \omega))^2)$ and $\chi^{12}(q, \omega) = J_{\perp}\chi_0(q, \omega)^2/(1 - (J_{\perp}\chi_0(q, \omega))^2)$. The crucial parameter controlling the susceptibilities in the static limit is

$$I_{\perp} \equiv J_{\perp}\chi_{max} = J_{\perp}\chi_0\xi^2. \quad (11)$$

Here χ_{max} is the maximum value of the in-plane spin susceptibility. We must assume $I_{\perp} < 1$ so that the material has no long range order. If $I_{\perp}^2 \ll 1$ then $\chi^{11} \approx \chi_0$ and $\chi^{12} \approx J_{\perp}\chi_0^2$. In this limit the interplane coupling has a weak effect and the RPA (which in this limit is just a perturbation expansion in J_{\perp}) is an appropriate model. On the other hand, if $I_{\perp}^2 \approx 1$ then the interplane coupling is strong and the use of the RPA may be questioned.

We now turn to the NMR experiments of interest. These are T_2 experiments performed on $\text{Y}_2\text{Ba}_4\text{Cu}_7\text{O}_{15}$, a material in which the single-chain structure of $\text{YBa}_2\text{Cu}_3\text{O}_7$ alternates with the double-chain structure of $\text{YBa}_2\text{Cu}_4\text{O}_8$ ^{2,22}. As a result, atoms on different planes of a bilayer have somewhat different local environments and therefore somewhat different NMR resonance frequencies, which may be independently studied. Despite the differences in local environment, the electronic properties of the two planes seem essentially identical – in particular, ratios of Knight shifts and in-plane relaxation rates are temperature-independent²². We therefore believe that the differences in observed relaxation rates and Knight shifts are due to differences in hyperfine couplings. An alternative view is that the electronic susceptibilities on the two planes differ. This difference may be included in our formalism and

analysis, and will not change the results in an important way (basically, one replaces χ^{11} by $(\chi^{11}\chi^{22})^{1/2}$).

Now the NMR T_2 measures the rate at which a nuclear spin is depolarized by interacting with other nuclear spins, i.e. it measures the nuclear-spin–nuclear-spin interaction strength. In high T_c materials the dominant contribution to the nuclear-spin nuclear-spin interaction comes from polarization of electronic spins, and may be related to the static limit of the real part of the electronic spin susceptibility²³. In $\text{Y}_2\text{Ba}_4\text{Cu}_7\text{O}_{15}$ it is possible to measure T_2 , the rate at which a spin in one plane is depolarized by spins in the same plane, and $T_{2\perp}$, the rate at which a spin in one plane is depolarized by spins in the other plane. T_2 is related to the electronic spin susceptibility by²⁴

$$\frac{1}{T_2^{(a)}} = \left[\sum_q [A_q^{(a)2} \chi_q^{11}]^2 - \left(\sum_q A_q^{(a)2} \chi_q^{11} \right)^2 \right]^{1/2} \quad (12)$$

while $T_{2\perp}$ is given by²⁵

$$\frac{1}{T_{2\perp}} = \left[\sum_q [A_q^{(1)} A_q^{(2)} \chi^{12}]^2 \right]^{1/2}. \quad (13)$$

Here we have allowed for the different hyperfine couplings in the two planes observed experimentally. We have calculated T_2 and $T_{2\perp}$ from Eqs. (10,12,13). The precise values obtained depend upon the form chosen for $f(q\xi, \omega = 0)$. We have used two forms for $f(x) \equiv f(q\xi, \omega = 0)$: a Lorentzian, $f(x) = 1/(1 + x^2)$, and a Gaussian, $f(x) = \exp(-\log(2)x^2)$ (the $\log(2)$ is introduced so $f(x = 1) = 1/2$). We measure ξ in units of the lattice constant, we set $\hbar = 1$ and assume that the hyperfine couplings can be approximated by their values at Q , A_Q^a . We find

$$\frac{1}{T_2^{(a)}} = A_Q^{(a)2} \chi_0 \xi g_{in}(I_\perp) \quad (14)$$

and

$$\frac{1}{T_{2\perp}} = A_Q^{(1)} A_Q^{(2)} J_\perp \chi_0^2 \xi^3 g_\perp(I_\perp) \quad (15)$$

where g_{in} and g_\perp are defined in terms of the function $f(x)$ via

$$g_{in}^2(I_{\perp}) = \frac{1}{2\pi} \left[\int_0^{\infty} dx \frac{f^2}{(1 - I_{\perp}^2 f^2)^2} - \frac{1}{2\pi\xi^2} \left(\int_0^{\infty} dx \frac{f^2}{1 - I_{\perp}^2 f^2} \right)^2 \right] \quad (16)$$

$$g_{\perp}^2(I_{\perp}) = \frac{1}{2\pi} \int_0^{\infty} dx \frac{f^4}{(1 - I_{\perp}^2 f^2)^2}. \quad (17)$$

In writing Eqs. 16,17 we have assumed that the correlation length is so long that lattice effects may be neglected. We have investigated this issue by performing the exact integrals numerically. The parameter governing the size of the lattice effects is $(\pi\xi)^{-1}$; for $\xi \geq 1$ we have found that lattice effects are negligible.

In Fig. 1 we present the calculated results for $\sqrt{T_2^{(1)}T_2^{(2)}}/T_{2\perp} = I_{\perp}g_{\perp}(I_{\perp})/g_{in}(I_{\perp})$. From the experimental values² $\sqrt{T_2^{(1)}T_2^{(2)}}/T_{2\perp} = 0.15$ at $T = 200$ K and $\sqrt{T_2^{(1)}T_2^{(2)}}/T_{2\perp} = 0.30$ at $T = 120$ K we obtain $I_{\perp} \approx 0.2$ at $T = 200$ K and $I_{\perp} \approx 0.4$ at $T = 120$ K. Note that even at the lowest temperature we find that the system is in the small I_{\perp} regime in which $T_2/T_{2\perp}$ is linear in I_{\perp} , suggesting that the between-planes coupling is sufficiently small that the RPA formula is justified.

The magnitude of J_{\perp} may be determined if χ_{max} is known and conversely. In the NMR and bulk susceptibility literature χ is defined in terms of the $[g\mu_B\vec{S}, g\mu_B\vec{S}]$ correlator, and results are presented as χ/μ_B^2 . This quantity differs by a factor of four from the susceptibility defined in this paper; we refer to it as χ^{exp} . If the susceptibility were only weakly q -dependent then the measured uniform susceptibility $\chi_{uniform}^{exp} \approx 2$ states/eV-Cu²⁶ would provide a good estimate for $4\chi_{max}$ and our value $I_{\perp} \approx 0.4$ would imply $J_{\perp} \approx 0.8$ eV. Such a value is very difficult to justify on microscopic grounds because the insulating antiferromagnetic parent compounds of the high T_c superconductors have in-plane exchange constants $J_{in-plane} \approx 0.12$ eV and, as shown in the previous section, $J_{\perp}/J_{in-plane} \sim 0.1$. It seems very unlikely that doping would lead to a $J_{\perp} \gg J_{in-plane}$. Therefore, we believe the cross-relaxation results imply $\chi_{max} \gg \chi_{uniform}$ in metallic, superconducting materials. A similar conclusion has been drawn from analyses of in-plane NMR^{9,23,10}, but these analyses required assumptions about magnitudes of hyperfine couplings and correlation lengths. These quantities drop out of the present analysis. The estimate $J_{\perp} \approx 10 - 20$ meV has been obtained from band

structure calculations²⁷, implying $\chi_{max}^{exp} \approx 80\text{-}160$ states/eV-Cu, while in Ref.²² the estimate $J_{\perp} \approx 25\text{meV}$ was presented.

We now turn to a more detailed discussion of the value of χ_{max} inferred from the discussion of the in-plane NMR. This discussion is based on the results contained in the recent paper of Barzykin and Pines¹⁰ which summarizes and analyzes a wide range of NMR data. (The results proposed in Ref.²⁸ lead to corrections which are smaller than our estimated uncertainties so we have not incorporated them). This paper is extremely useful, but has a few limitations: in particular, explicit error estimates are not given, and the analysis for $\text{YBa}_2\text{Cu}_3\text{O}_{6.63}$ does not include interplane effects argued below to be important. We believe the uncertainties in values for $\text{YBa}_2\text{Cu}_3\text{O}_{6.63}$ are substantial and difficult to estimate with accuracy.

Barzykin and Pines show that once the hyperfine coupling is determined, the measured in-plane T_2^{-1} rate is proportional to the quantity χ_{max}/ξ . Their Table I and Fig. 2 gives for $\text{YBa}_2\text{Cu}_3\text{O}_7$ the estimate $\chi_Q^{exp}(T = 100\text{K})/\xi = 30$ states/eV-Cu. We believe 10% uncertainties in hyperfine couplings are reasonable²⁹, implying 20% uncertainties in χ_{max}^{exp}/ξ . To obtain an estimate for χ_{max} an estimate for ξ is required. We argued²⁹ that the uncertainties in the NMR estimate for ξ are large; we suggested, on the basis of earlier data, that for $\text{YBa}_2\text{Cu}_3\text{O}_7$ at $T=100\text{K}$ a plausible estimate is $0.5 \lesssim \xi \lesssim 2$ with the most likely value $\sim 1 - 1.5^4$. From Fig. 14 and Fig. 16 of Ref.¹⁰, which are based on more recent data, one obtains the larger estimates $\xi/a = 1.9 - 2.3$. For $\text{YBa}_2\text{Cu}_3\text{O}_{6.6}$ it seems clear that ξ must be larger than in $\text{YBa}_2\text{Cu}_3\text{O}_7$; The analysis of Ref.¹⁰ yields $\xi/a(T = 100\text{K}) = 7.4$. This value seems to us too large, but regardless of the precise value of ξ , it is clear that the larger T_2^{-1} and presumably larger ξ implies that χ_{max} in $\text{YBa}_2\text{Cu}_3\text{O}_{6.63}$ is larger by a factor at least of order four than in $\text{YBa}_2\text{Cu}_3\text{O}_7$. We thus roughly estimate that χ_{max}^{exp} in $\text{YBa}_2\text{Cu}_3\text{O}_7 \sim 50$ states/eV-Cu (with \sim factor of two uncertainties) and χ_{max}^{exp} in $\text{YBa}_2\text{Cu}_3\text{O}_{6.63}$ is at least 250 states/eV-Cu (with rather larger uncertainties). The value obtained from the results in Ref.¹⁰ is $\chi_{max}^{exp} \sim 440$ states/eV-Cu. As previously remarked, $\text{Y}_2\text{Ba}_4\text{Cu}_7\text{O}_{15}$ has a doping intermediate between the two materials, but probably closer to O_7 . The previously derived

estimate $\chi_{max}^{exp} \sim 80 - 160$ states/eV-Cu is thus consistent with the results of the in-plane NMR, so it is likely that the effective between-planes coupling does not change much with doping.

The rapid dependence of χ_{max} with doping inferred from in-plane NMR measurements suggest that for $\text{YBa}_2\text{Cu}_3\text{O}_{6.63}$ and lower dopings, χ_{max} is so large that $I_{\perp} \approx 1$. For these materials the planes are thus very strongly coupled at low energies. The simple RPA formula we have used is unlikely to be accurate, and the between-planes coupling must be taken into account in interpreting even in-plane NMR experiments. A preliminary attempt along these lines has appeared²¹.

In summary, the cross-relaxation experiment shows that the real part of the susceptibility at some non-zero wavevector q is much larger than the uniform susceptibility. The temperature dependence of the T_2 rates must be due to the temperature dependence of this antiferromagnetic maximum. Two scenarios have been proposed for the temperature dependence: in the *antiferromagnetic scenario* the temperature dependent quantity is the correlation length ξ . In the *generalized marginal Fermi liquid scenario* the temperature dependent quantity is the overall amplitude $\bar{\chi}$ ³⁰. From Eqs. (14,15) we see that in the regime where $T_{2\perp}$ is linear in I_{\perp} the antiferromagnetic scenario predicts $T_2^3/T_{2\perp}$ is temperature independent, while the marginal Fermi liquid scenario predicts $T_2^2/T_{2\perp}$ is temperature independent. The experimentally determined ratios are plotted in Fig. 2 and are more consistent with the antiferromagnetic scenario.

The imaginary parts of the two independent susceptibilities χ_{even} and χ_{odd} are measurable via neutron scattering because they have different dependences on q_z , the momentum transverse to the CuO_2 planes¹. Neutron scattering experiments have been performed on a variety of metallic members of the yttrium-barium family of high- T_c materials^{1,12,31}. The experimental result is that *only* χ_{odd} is seen. At frequencies less than 30 meV and temperatures less than room temperature the even parity fluctuations are claimed to be completely frozen out. The theory of neutron scattering in high T_c materials is presently controversial. There is no generally accepted model which correctly accounts for the observed lineshapes

and temperature dependences. To investigate the connection between the cross-relaxation experiments and neutron scattering we have chosen to calculate the ratio of the q -integrated even and odd parity susceptibilities. This ratio is insensitive to the precise details of the susceptibilities. For definiteness we used the “MMP”, dynamical exponent $z = 2$ ansatz $\chi_0(q, \omega) = \bar{\chi}/(\xi^{-2} + q^2 - i\omega/\Gamma)$. Here Γ is a microscopic spin relaxation time. The results depend on I_\perp and on $\omega_{SF} = \Gamma/\xi^2$, which we define here to be the softest spin fluctuation frequency of a single plane. Of course the between-planes coupling will reduce this frequency for the odd parity channel and increase it for the even channel. Results are shown in Fig. 3 for several values of I_\perp . We see that the relative weight of the even parity fluctuations becomes small only for $I_\perp > 0.5$. We believe that the neutron results, which seem to require a $I_\perp > 0.5$, are not in contradiction to our analysis of the cross-relaxation experiment, which yielded a $I_\perp \leq 0.4$, because the strongest neutron evidence for locked bilayers was obtained from a study of $\text{YBa}_2\text{Cu}_3\text{O}_{6.5}$ ¹, which as we have previously noted is much closer to the magnetic instability than $\text{Y}_2\text{Ba}_4\text{Cu}_7\text{O}_{15}$, and therefore may be expected to have $I_\perp \sim 1$.

As a side remark we note that a recent neutron scattering work provided a bound on the magnetic scattering in $\text{YBa}_2\text{Cu}_3\text{O}_7$ ¹¹. Bearing in mind the factor of $(g^2\pi/2)$ difference between NMR and neutron conventions discussed above, we note that the upper bound implied by the neutron experiment for $\text{YBa}_2\text{Cu}_3\text{O}_7$ is $\chi_{max}^{exp} < 300$ states/eV-Cu. This bound is comfortably larger than the NMR estimates obtained by interpreting in-plane NMR experiments. At this time, therefore, there is no evidence of a contradiction between neutron scattering experiments and the “MMP” scenario for interpreting the NMR.

IV. SUPERCONDUCTING STATE

Another experiment relevant to bilayer coupling in the Y-Ba system is the observation of a sharp peak at an energy of 41 meV in the antisymmetric susceptibility of *superconducting* $\text{YBa}_2\text{Cu}_3\text{O}_7$ ¹². A corresponding peak in the *symmetric* channel has not been observed^{12,11}, and an upper bound on the intensity in the symmetric channel of about 30% of the inten-

sity in the antisymmetric channel has been established¹¹. A number of theoretical works have investigated this peak (see, e.g.^{16,18,32,33} and references therein). We believe that the most likely explanation is that the peak is a collective mode pulled down below the superconducting gap edge by interactions, and that its appearance only in the antisymmetric channel is due to the non-zero J_{\perp} . This explanation is essentially that given by Liu et al.¹⁶ (although they did not interpret their results – which were basically numerical – in precisely this manner). An objection to this interpretation was raised by Mazin and Yakovenko¹⁸, who argued that within such theories an observable peak should also exist in the symmetric channel. In the remainder of this section we present a simple RPA theory of the 41 meV mode. Although the RPA is presumably not quantitatively accurate it is in fact the basis of most previous work (^{16–18}) and is to some extent analytically tractable. Our treatment gives insight into the results of¹⁶, shows why the effect was not seen by¹⁷ and shows that the objection of¹⁸ is unfounded.

The fundamental object in the RPA is the bare electron polarizability χ_{00} . This is given, at $T = 0$ in a superconductor, by e.g. Eq. 1 of Ref.¹⁸ (although one must multiply their expression by 2 to convert to our conventions). In two spatial dimensions the constraints that the initial and final states lie on the Fermi surface completely specifies the kinematics (up to discrete lattice symmetry operations). Thus the threshold behavior of χ'' for frequencies near the gap edge may be found analytically. For $Q = (\pi, \pi)$ and bearing in mind that $2Q$ is a reciprocal lattice vector one finds

$$\begin{aligned} \chi_{00}(Q, \omega) &= \chi_{00}^{\text{reg}} + \frac{4}{\pi} \frac{\sqrt{|\Delta_{p_0} \Delta_{p_0+Q}|}}{v_{p_0} v_{p_0+Q} \sin \theta} \log \left| \frac{\sqrt{|\Delta_{p_0} \Delta_{p_0+Q}|}}{\omega - \Delta_{p_0} - \Delta_{p_0+Q}} \right| \\ &\equiv \chi_{00}^{\text{reg}} \left[1 + A \log \left| \frac{\sqrt{|\Delta_{p_0} \Delta_{p_0+Q}|}}{\omega - \Delta_{p_0} - \Delta_{p_0+Q}} \right| \right] \end{aligned} \quad (18)$$

Here p_0 is a wavevector such that $\epsilon_{p_0} = \epsilon_{p_0+Q} = 0$, θ is the angle between \vec{v}_{p_0} and \vec{v}_{p_0+Q} and it is assumed that the Fermi surface does not pass through a van Hove point (so $v_{p_0} \neq 0$) and $\theta \neq 0, \pi$. χ_{00}^{reg} is a function which is not singular at the gap edge; one expects χ_{00}^{reg} to be basically equal to the normal state susceptibility, and $A \sim (\Delta/E_F)$. Of

course, as the Fermi surface approaches the van Hove point, A increases. The dispersion $\epsilon_p = -2t(\cos p_x + \cos p_y) + 4t' \cos p_x \cos p_y - \mu$ with $t' = t/2$ and $\mu = -1.5t$ has been claimed to describe $\text{YBa}_2\text{Cu}_3\text{O}_7$ ³⁴. For this dispersion $\chi_{00}^{\text{reg}} = 0.6/t$ and $A = 0.8(\Delta/t)$. Thus using $t \approx 0.2\text{eV}$ and $\Delta \sim 20 \text{ meV}$, we estimate $A \sim 0.1$. The coefficient of the logarithm is quite sensitive to details of band structure, thus the significance of this estimate is that it may be reasonable to assume A is small, but not absurdly so. Note, though, that a key feature of the calculation is that at p_0 and $p_0 + Q$ the superconducting gap is at or near its maximum, so that A is maximal and there is no quasiparticle damping. Other workers (including¹⁷) have studied a model with $t' = 0$. For this model, p_0 and $p_0 + Q$ are near gap minima, so A is very small and the damping is large, so the effects we will discuss below will not be observable. Thus it may be concluded that within the present theory the 41 meV peak is very sensitive to details of band structure and gap anisotropy.

The RPA formula $\chi^{(a,s)} = \chi_{00}/(1 - (J \pm J_{\perp})\chi_{00})$ and Eq. 18 thus imply that the susceptibility diverges at frequencies $\omega^{a,s}$ given by

$$2\Delta_{p_0} - \omega^{a,s} = 2\Delta_{p_0} \exp \left[-\frac{1 \mp I_{\perp}}{(J \pm J_{\perp})\chi_{max}A} \right] \quad (19)$$

Here $\chi_{max} = \chi_{00}/(1 - J\chi_{00})$ and $I_{\perp} = J_{\perp}\chi_{max}$ have the same meaning as in section 3. One sees immediately that if the system is not too far from a magnetic instability the large value of $J\chi_{max}$ may compensate for the small value of A . Also, the argument of the exponential differs for the symmetric $(1 + I_{\perp})/(J - J_{\perp})$ and antisymmetric $(1 - I_{\perp})/(J + J_{\perp})$ cases. If $J\chi_{max}A < 1$ and I_{\perp} is not too small, then only the antisymmetric pole is appreciably removed from the gap edge. Finally, the weight in the resonance, $I^{\pm} = \int d\omega \chi''$, may be written approximately

$$I^{a,s} = \frac{4\pi(2\Delta_{p_0} - \omega_{a,s})}{JA} \quad (20)$$

The weight scales with the difference in energy from the gap edge, and is thus much smaller for the symmetric mode. It is enhanced by the factor $1/A \sim 10$. Because precise values for the various quantities are not available it is difficult to compare our estimate

of the weight precisely to experiment. In Ref.¹⁶ the value $J \sim 80$ meV was used³⁴. The conventions are those of this paper, so to convert I to the units used in¹¹ one must multiply by $2/\pi$. The result is $I^{a,s} \sim 40 (1 - \omega^{a,s}) 2\Delta_{p_0}$. It thus seems that weights of order unity or larger in the antisymmetric channel are not difficult to obtain.

V. CONCLUSIONS

We have given expressions which may be useful in interpreting experiments relating to bilayer coupling in $\text{YBa}_2\text{Cu}_3\text{O}_{6+x}$. We have determined the quantum correction to the optic magnon gap in the insulator, and given the theory of the NMR cross relaxation T_2 experiment. We have shown that a $J_\perp \approx 14$ meV is roughly consistent with all experiments, and that the cross-relaxation experiment implies that χ has a very substantial antiferromagnetic peak, which however is not large enough to have been observed in recent neutron experiments.

We have shown that a $J_\perp \approx 14$ meV is consistent with neutron scattering experiments and with an extension to the bilayer system of the widely - used ‘‘MMP’’ analysis^{9,10} of NMR. We have also noted that there is at present no obvious contradiction between neutron scattering and the MMP scenario for NMR. We have proposed an explanation for the 41 meV peak observed in the superconducting state of $\text{YBa}_2\text{Cu}_3\text{O}_7$ and have argued that in the Y-Ba system at dopings corresponding to $\text{YBa}_2\text{Cu}_3\text{O}_{6.63}$ interplane effects will have a significant effect on the low-energy magnetic dynamics of the underdoped materials. Understanding the effects is a crucial problem for future research.

We thank T. M. Rice, R. Stern and M. Mali for helpful discussions of NMR, M. Takigawa for drawing our attention to the difference between NMR and neutron conventions, D. Pines for a critical reading of the manuscript, B. Keimer for discussions of the neutron experiments, D. A. Huse for discussion of the $S = 1/2$ Heisenberg model, H. Fukuyama for discussions of RPA calculations and K. Levin, Q. Si and Y. Zha for discussions of Ref.¹⁶. HM acknowledges the hospitality of AT&T Bell Laboratories where this work was begun and AJM and HM

thank the Institute for Theoretical Physics in Santa Barbara where it was completed.

*Address after Sept 1, 1996: Department of Physics, The Johns Hopkins University,
Baltimore MD 21218.

REFERENCES

- ¹ J. M. Tranquada, G. Shirane, B. Keimer, S. Shamoto and M. Sato, Phys. Rev. **B40**, 4503 (1989) and Phys. Rev. **46**, 5561 (1992).
- ² R. Stern, M. Mali, J. Roos et. al., Phys. Rev. **B52**, 15734 (1995).
- ³ B. L. Altshuler and L. B. Ioffe, Solid State Communications **82**, 253 (1992).
- ⁴ A. J. Millis and H. Monien, Phys. Rev. Lett. **70**, 2813 (1993).
- ⁵ B. L. Altshuler, L. B. Ioffe, A. I. Larkin and A. J. Millis, JETP Lett. **59**, 65 (1994).
- ⁶ M. Ubbens and P. A. Lee, Phys. Rev. **B50**, 438 (1994).
- ⁷ B. L. Altshuler, L. B. Ioffe and A. J. Millis, Phys. Rev. **B53**, 415 (1996).
- ⁸ M. Takigawa et al., Phys. Rev. **B42**, 243 (1991).
- ⁹ A. J. Millis, H. Monien and D. Pines, Phys. Rev. **B42**, 167 (1990).
- ¹⁰ V. Barzykin and D. Pines, Phys. Rev. **B52**, 13585 (1995).
- ¹¹ H. F. Fong, B. Keimer, D. Reznik, D. L. Milius and I. A. Aksay, unpublished.
- ¹² H. A. Mook, M. Yethraj, G. Aeppli, T. E. Mason and T. Armstrong, Phys. Rev. Lett. **70**, 3490 (1993).
- ¹³ A. J. Millis and H. Monien, unpublished (cond-mat/9506088).
- ¹⁴ D. Reznik, P. Bourges, H. F. Fong, L. P. Regnault, J. Bossy, C. Vettier, D. L. Miller, I. A. Aksay and B. Keimer, unpublished.
- ¹⁵ S. M. Hayden, G. Aeppli, T. G. Perring, H. A. Mook and F. Dogan, unpublished.
- ¹⁶ D. L. Liu, Y. Zha and K. Levin, Phys. Rev. Lett. **75**, 4130 (1995).
- ¹⁷ B. Normand, H. Kohno and H. Fukuyama, J. Phys. Soc. Jpn. **64**, 3903 (1995).
- ¹⁸ I. I. Mazin and V. M. Yakovenko, Phys. Rev. Lett. **75**, 4134 (1995).

- ¹⁹ D. Arovas and A. Auerbach, Phys. Rev. Lett. **61**, 617 (1988).
- ²⁰ R. R. P. Singh and D. A. Huse, Phys. Rev. **B40** 7247 (1989).
- ²¹ A. J. Millis and H. Monien, Phys. Rev. **B50** 16606 (1994).
- ²² R. Stern, M. Mali, I. Mangelschots, J. Roos, D. Brinkmann, J-Y. Genoud, T. Graf and J. Muller, Phys. Rev. **B50**, 426 (1994).
- ²³ C. H. Pennington and C. P. Slichter, Phys. Rev. Lett. **66**, 381 (1991).
- ²⁴ D. Thelen and D. Pines, Phys. Rev. **B49**, 3528 (1994).
- ²⁵ H. Monien and T. M. Rice, Physica **C235-240**, 1705 (1994).
- ²⁶ R. E. Walstedt et. al., Phys. Rev. **B45**, 8074, (1992).
- ²⁷ O. K. Andersen et. al. Phys. Rev. **B49**, 4145 (1994).
- ²⁸ Y. Zha, V. Barzykin, D. Pines, Phys. Rev. **B**, August 96, in press
- ²⁹ A. J. Millis and H. Monien, Phys. Rev. **B45**, 3059 (1992).
- ³⁰ Q. M. Si, Int. J. of Mod. Phys. **B8**, 47 (1994).
- ³¹ J. Rossat-Mignod et al., Physica **C185**, 86 (1991).
- ³² E. Demler and S.-C. Zhang, Phys. Rev. Lett. **75**, 4126 (1995).
- ³³ H. Kohno, B. Normand and H. Fukuyama, to appear in *Proceedings of the 10th Anniversary HTS Workshop on Physics, Materials and Applications*.
- ³⁴ Q. Si and Y. Zha, private communication.

FIGURES

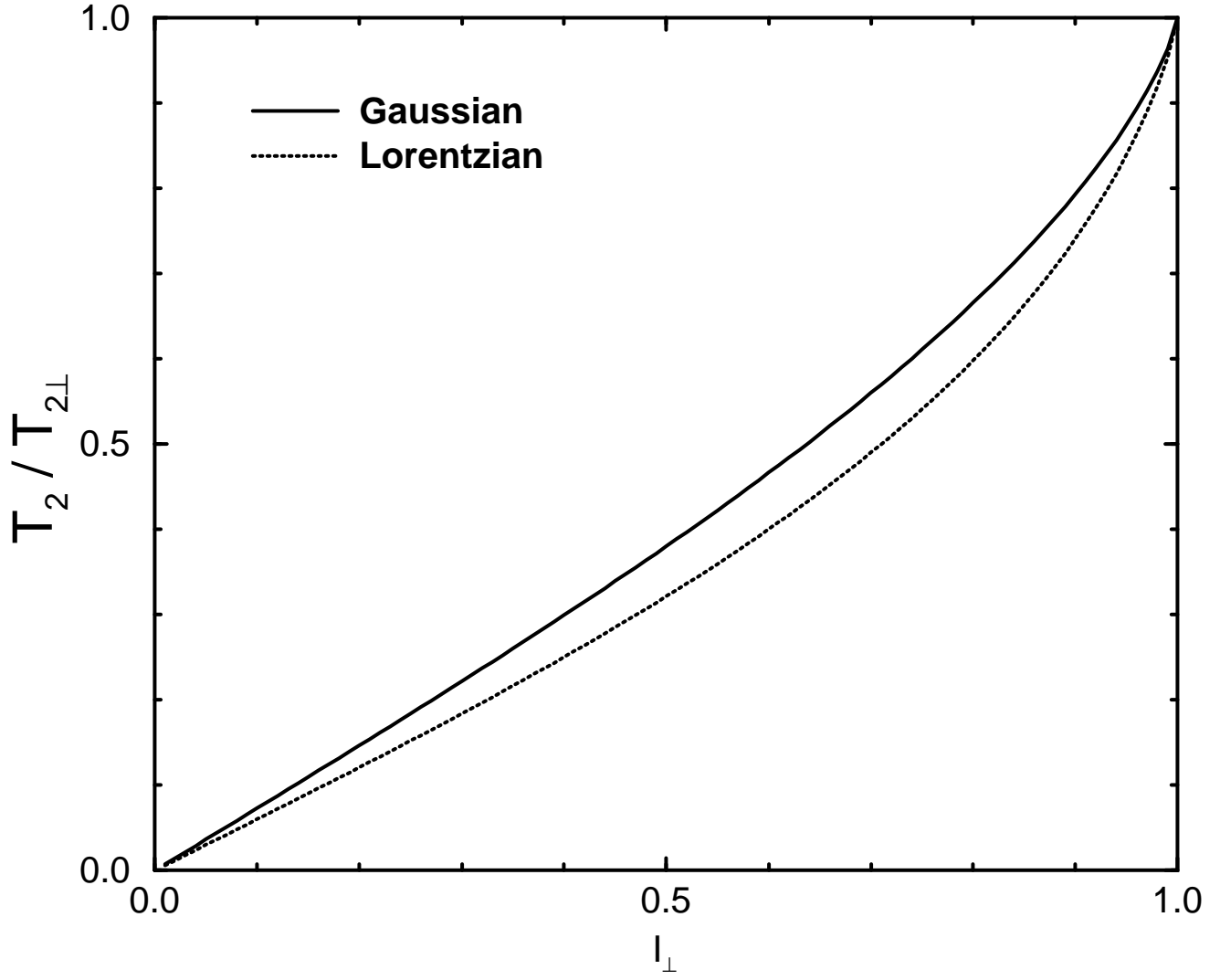


FIG. 1. Ratio of cross-relaxation rate $1/T_{2\perp}$ to in-plane relaxation rate $1/T_2$ plotted versus coupling parameter $I_\perp = J_\perp \chi_{max}$ for Lorentzian (dotted line) and Gaussian (solid line) form factors and calculated from Eqs. (6-9).

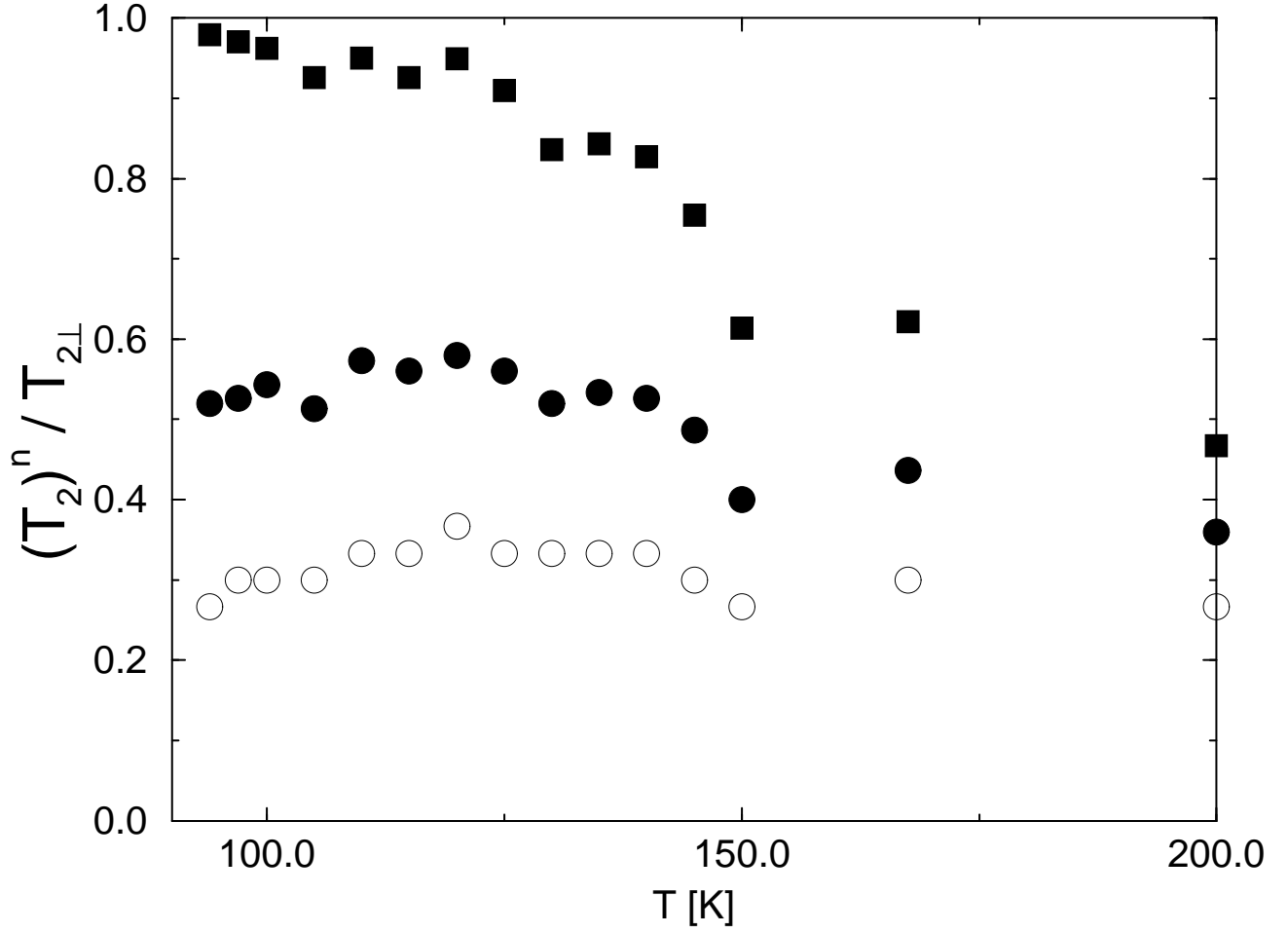


FIG. 2. Experimentally determined ratio of $1/T_{2\perp}$ to n th power of $1/T_2$ for $n=1$ (\square), 2 (\bullet), 3 (\circ) in arbitrary units. That the $n=3$ (\circ) curve has less temperature dependence than the $n=2$ (\bullet) curve suggests the existence of a growing magnetic correlation length.

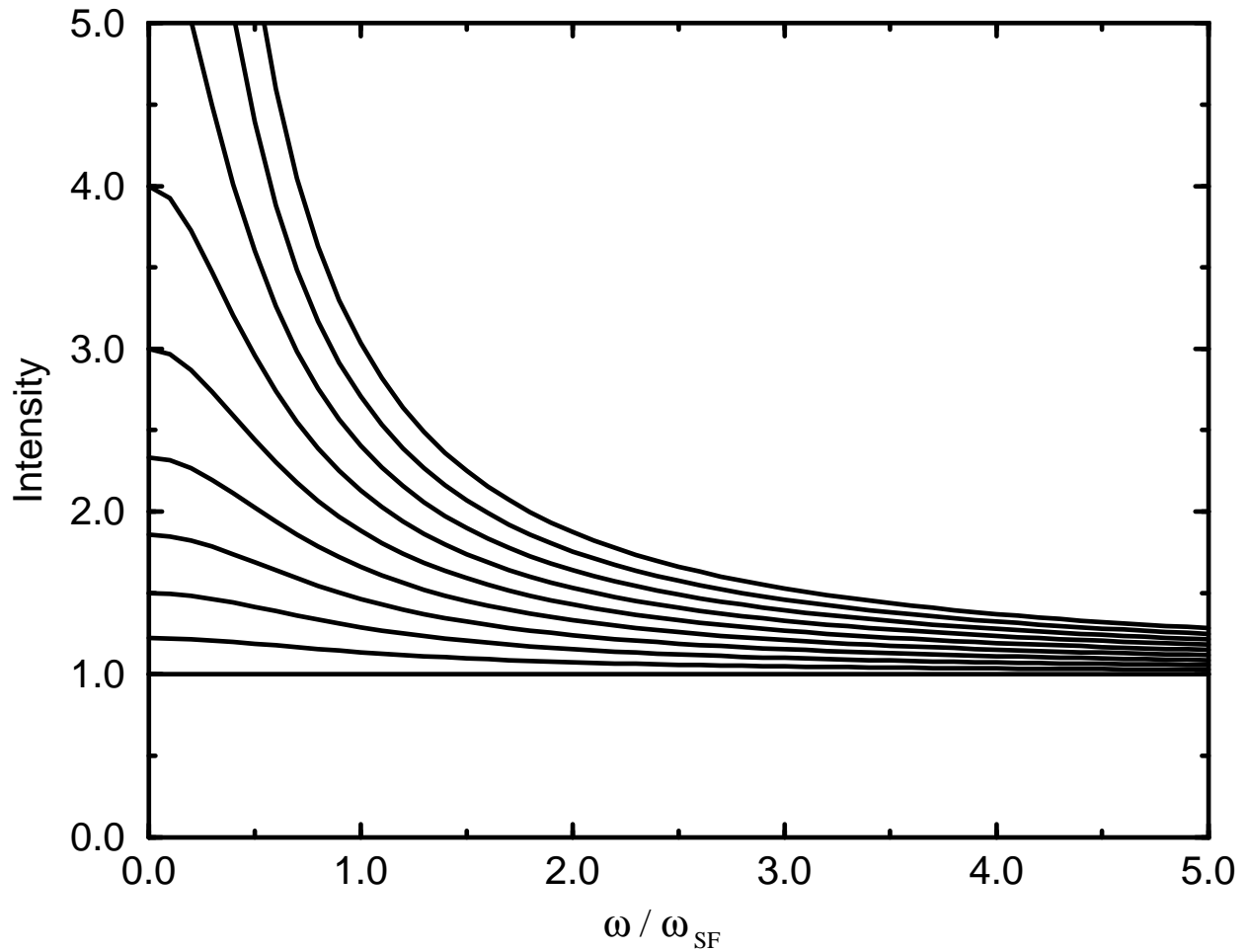


FIG. 3. Calculated ratio of q -integrated odd-parity neutron absorption to q -integrated even parity neutron absorption, plotted versus frequency for $I_{\perp} = J_{\perp} \chi_{max} = 0.0, 0.1 \dots 0.9$. $I_{\perp} = 0.0$ corresponds to the lowest curve and $I_{\perp} = 0.9$ to the top curve.